Electric characterization of a Bioinspired Gripper

Caracterización Eléctrica de una Pinza Bioinspirada

Alan Jesús Estrada Cabrera[1] (ID), Margarita Tecpoyotl-Torres[*2] (ID),
Pedro Vargas-Chable[2,3] (ID) y Ramón Cabello-Ruiz[3] (ID)

[1]Maestría en Ingeniería y Ciencias Aplicadas, MICA, Universidad Autónoma del Estado de Morelos, UAEM
Av. Universidad 1001, Col. Chamilpa. Cuernavaca, Morelos, C.P. 62209. México
alan.estradac@uaem.edu.mx
[2]Centro de Investigación en Ingeniería y Ciencias Aplicadas, CIICAp, UAEM
Av. Universidad 1001, Col. Chamilpa. Cuernavaca, Morelos, C.P. 62209. México
[*]tecpoyotl@uaem.mx, pedro.vargas@uaem.mx
[3]Facultad de Ciencias Químicas e Ingeniería, FCQeI, UAEM
Av. Universidad 1001, Col. Chamilpa. Cuernavaca, Morelos. C.P. 62209. México
ramon.cabello@uaem.edu.mx

ABSTRACT

This work focuses on a normally open bioinspired microgripper, which corresponds to the Microelectromechanical Systems (MEMS) field, as well as on its scaling and fabrication process in aluminum 6053 for performance testing. The design was inspired by the mandibles of ants. Its structure is composed of a flexible M-type amplifier and a Z-shaped chevron actuator. The design and simulation were performed using ANSYSTM. The aluminum resistivity and the equivalent resistance of the gripper were calculated, and experimental tests were carried out with an inductor (L), capacitor (C) and resistor (R) electrical property meter, LCR. Experimental characterization of the gripper was carried out, applying a sweep of electric current from 5 up to 60 A to the actuator. The temperature values were registered using a thermographic camera; the displacement was determined using a microscope. The average error between numerical and experimental results of the actuator shaft temperature is lower than 13%.

RESUMEN

Este trabajo se enfoca en una micropinza bioinspirada, normalmente abierta, que corresponde al campo de los sistemas microelectromecánicos, MEMS, así como en el escalamiento del dispositivo y su proceso de fabricación en aluminio 6053 para la realización de pruebas de desempeño. El diseño está inspirado en las mandíbulas de las hormigas. Su estructura se compone de un amplificador flexible de tipo M y un actuador chevrón con vigas de forma Z. El diseño y la simulación se realizaron con ANSYSTM. Se calcularon la resistividad del aluminio y la resistencia equivalente de la pinza, y se realizaron pruebas experimentales con un medidor de propiedades eléctricas de inductores (*L*), capacitores (*C*) y resistencias (*R*), LCR. Se realizó la caracterización experimental de la pinza, aplicando un barrido de corriente eléctrica desde 5 hasta 60 A al actuador. Los valores de temperatura se registraron mediante una cámara termográfica; el desplazamiento se determinó con un microscopio. El error promedio entre los resultados numéricos y experimentales de la temperatura de la flecha del actuador son menores al 13%.

1. INTRODUCTION

Microgripper are devices that belong to the field of Microelectromechanical Systems (MEMS), they are tools that in recent years have acquired a great development mainly in specific applications such as microassembly [1], robotics [2], microelectronics [3], among the best known. MEMS due to their accelerated development have expanded in many fields such as microfluidics and microacoustics, generating biomedical devices, microreactors and microrockets, among others. This has allowed the creation of new MEMS subfields, such as BioMEMS, PowerMEMS and RF MEMS, among the best known [4].

In this work it is proposed, from the design of the micromanipulator device, to perform the scaling to carry out its fabrication at macro scale level, as a technique to experimentally validate the analyses developed in the simulation, as has been reported in [5]. This, as an alternative when there are limitations and microfabrication and testing at the micrometer level cannot be performed.

To design the gripper is based on the biomimetic design spiral [6], which is a methodology that provides a concise description of the essential elements of a design process that uses nature as a guide to create solutions (Figure 1).
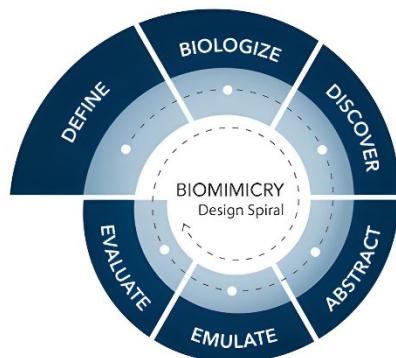

Figure 1. Graphical representation of the biomimetic design spiral [6].

There are three levels of Biomimetics, the first one consists of imitating the natural form, the second level involves the imitation of a natural process, in the third level, the imitation of natural ecosystems and is classified as deep biomimicry, as can be seen in Figure 2. The microgripper shown here is in the first level, since the morphology of an insect is considered as a source of inspiration [7], [8].

Bio-inspiration has been implemented in MEMS technology where microgrippers inspired from biological systems called soft tweezers have been developed, as they feature a stimuli-sensitive soft grip [9].

The microgripper presented here is actuated by an electrothermal Z-arm chevron. To carry out its operation, current is generally passed through the arms to cause resistive heating [7], thus generating a uniform linear motion in the shaft, which drives the arms of the microgripper generating its opening.

Figure 2. Biomimetics levels [8].
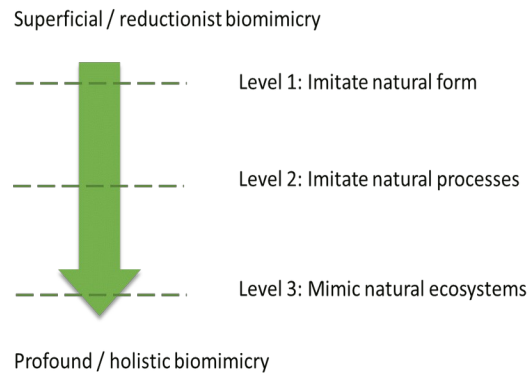
The structure of this article is as follows: In Section 1, a brief introduction to MEMS and Bio-inspiration is presented. In section 2, the design and electrical modeling of the clamp is shown. In Section 3, the simulations performed are shown. The fabrication process is described in Section 4. Experimental tests are presented in Section 5, while conclusions are shown in Section 6.

2. GRIPPER DESIGN AND ELECTRICAL MODELING

Several attempts were made to carry out the design of the microgripper inspired by the mandibles of an ant. Figure 3a shows the morphology of the jaws taken as inspiration and the structural interpretation of the mechanism. It was determined that the design shown in Figure 3b, showed adequate force and displacement performance parameters. This gripper design was improved by parameterization. It was found that, by enlarging the size of the arms, at certain points its performance was favored.

(a)

(b)
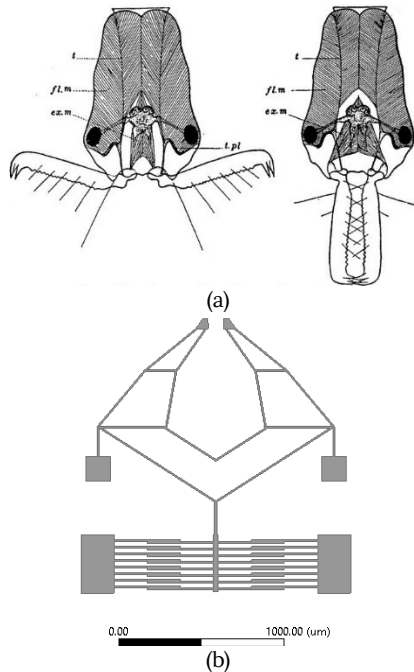
Figure 3. (a) Musculature of the head of an ant Odontomachus hastatus (Public domain image) and (b) structure of the microgripper for simulation and fabrication.

2.1. Design of the microgripper with scaling

The dimensions of the structure were developed for implementation using Silicon On Insulator (SOI) wafers and were proposed based in [10], [11].

To validate the performance of the geometry, scaling was performed, and the following considerations were made:

- Structural material: The design with scaling is implemented in aluminum plates.
- Scaling: Dimensions were scaled with a factor 1:100 only on the surface. Thickness is determined only considering the commercial aluminum plate availability. The thickness was 1mm. The latter, according to the availability of aluminum plate thickness.
- Holes: They were integrated in anchors for the fastening of the structure in the experimentation.

The total dimensions of the microgripper in micrometer scale are 1630x1656x70 μm. After doing the scaling and some additional adjustments on the size of the anchors, in mesometric scale it is 153x166.75x1 mm. Figure 4 shows the dimensions and dimensions of the left half of each of the two sections that make up the clamp, that is, the actuator and the clamping mechanism. Descriptions and dimensions are presented in Table 1.

(a)

(b)
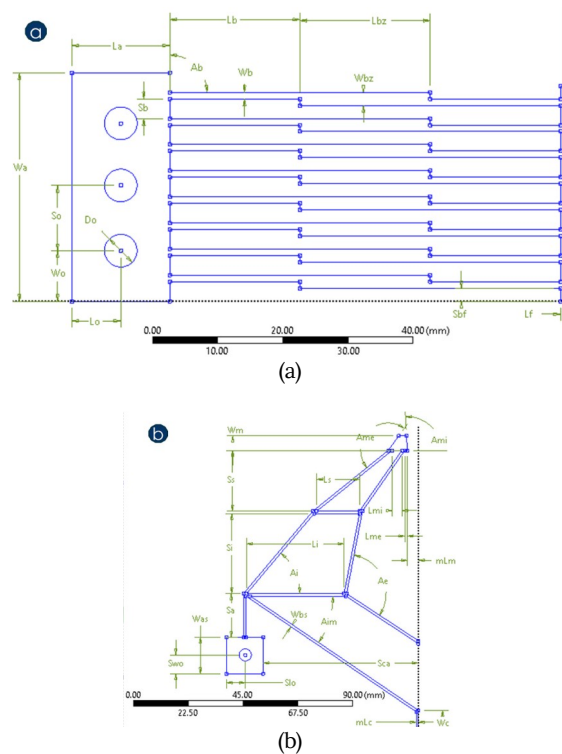
Figure 4. Geometry coordinates of the left half (a) of the chevron Z actuator and (b) of the clamp.

Table 1. Dimensions of the gripper elements.

ID	Description	Magnitude (mm)
L_a	Anchor length	20
W_a	Anchor width	35
L_f	Shaft length	15
W_f	Shaft width	35
L_b	Beam length	20
W_b	Beam width	1
S_b	Beams distance	3
L_{bz}	Length of Z-shaped section of beam	20
W_{bz}	Width of Z-shaped section of beam	2
h	Beam thickness	1
S_{ca}	Separation between the square clamp anchor and the center	63.75
W_c	Connecting beam anchor between actuator and clamping section	20.69
mLc	Half-length of connecting beam	0.75
mLm	A half sepation between jaws	4.5
L_{me}	Length of external jaw	1
L_{mi}	Length of lower jaw	4
W_m	Jaw width	6
W_{hs}	Beams length of clamp	1
S_s	Separation between upper arm and jaws	25
L_s	Length of upper beam	17.5
S_i	Separation between upper and lower beams	33
L_i	Length of lower beam	40
S_a	Separation between upper beam and anchor	18
W_{as}	Width of anchor of clamping section	15
S_{wo}	Clearance between square anchor shore and hole	7.75
S_{lo}	Clearance between square anchor shore and hole	7.75

ID	Description	Magnitude (°)
A_b	Angle between beams and anchors (chevron actuator)	90
A_{mi}	Inner angle of the jaws	93
A_{me}	outer angle jaws	165
A_e	Outer angle	112.5
A_i	Inner angle	50
A_{im}	Internal angle of the M-shaped amplifier	34.2

2.2. Electrical modeling of gripper

The equations used for the electrical characterization are shown in Table 2.

Table 2. Equations for electrical characterization.

|	Equations		Variable description
Ohm Law	$V = IR$, (V)	(1)	
Resistance	$R = \rho \frac{l}{A}$. (W)	(2)	I: Current magnitude, (A)
Electric current density	$J = \frac{I}{A}$. (A/m²)	(3)	ρ: Resistivity, ($\Omega{\cdot}m$) l: Device length, (m)
Electric field magnitude	$E = \frac{V}{l}$, (V/m)	(4)	A: Cross section area, (m^2)

2.3. Gripper resistance

2.3.1. Z-shaped chevron actuator

The resistive analysis on the actuator was carried out based on Ohm's Law, equation 1. Equation 2 was also used.

The resistive analysis of the complete actuator (series of resistances corresponding to each of its halves) resulted in equation 5, which provides the total resistance of the chevron actuator.

$$R_{TA} = \frac{1}{4\,W_a\,t}\left(\frac{\rho\left(8\,L_a\,W_b\,W_z + W_a\left(2\,L_b\,W_z + L_z\,W_b\right)\right)}{W_b\,W_z} \right) \qquad (5)$$

Substituting the required magnitudes in Equation 5, a resistance of 555 μΩ is obtained.

(a)

(b)
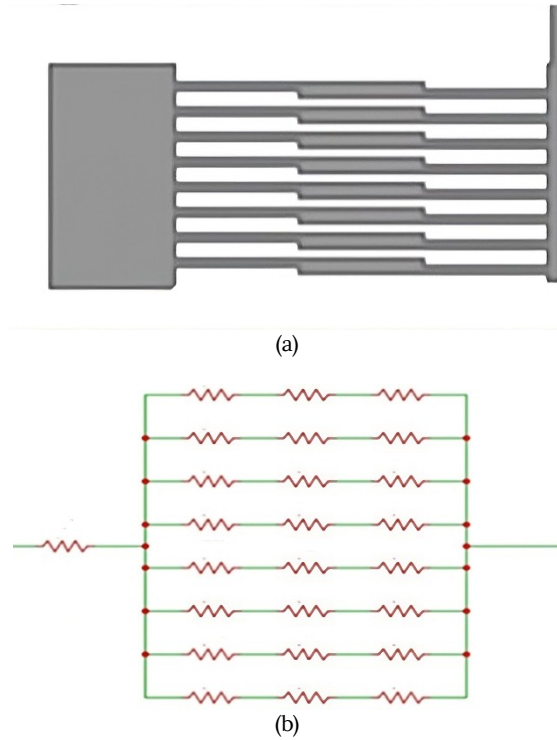
Figure 5. (a) Geometry, and (b) Resistive model of the left half of Z-shaped chevron actuator.

2.3.2. Gripper resistance

The calculation of the gripper resistance is equivalent to that of the Z chevron actuator. This is since each arm of the manipulation section is coupled to the shaft of the Z-shaped actuator and is not attached to another section, which allows us to observe that it is a resistive element with a single connection at one of its ends, that is, each arm emulates a resistor in open circuit, so it does not impact the total resistive value.

3. SIMULATION RESULTS

The gripper was simulated by finite element method with the Ansys Workbench software using the Steady State Thermal, Thermal Electric and Static Structural tools. A power source was applied that corresponds to a sweep in electric current intensity from 5 up to 60 A with steps of 5 A in the actuator anchors.

The room temperature with which the experimental tests were carried out for 6 days showed variations from 21 to 24 °C, as shown below. It should be noted that the simulations were repeated with the value measured on each day to reduce the errors between the numerical and experimental results. From the simulation, the temperature distribution and deformation were obtained, which are the performance parameters on which this work focuses.

Electric simulation was performed with the parameters shown in Table 3.

Table 3. Electrical properties of the aluminum-implemented gripper.

Parameters and units	Aluminum	Source
Resistivity, ρ (Ω ·m), at 24 °C	4.33E-8	Experimentally obtained
Electric conductivity, (W/(m/°C))	163	[12]

It should be noted that the magnitude of the resistivity was obtained from experimental tests in the laboratory with an LCR meter and a rectangular specimen of this material. The procedure is described in section 4.

3.1. Boundary conditions for numerical analysis

To carry out the performance analysis of the gripper, the boundary conditions required in Steady State Thermal are applied. These conditions are:

- A current source from 5 up to 60 A is applied to one of the anchors (on the right in Figure 6) of the chevron actuator, by parameterization.

- 0 V is applied to the left anchor, emulating a ground connection.
- Each anchor of the actuator and gripper arms was assigned at room temperature, which corresponded to the room temperature recorded on the different days.

Figure 6, on the left, shows the simulation tree and the assignment elements that are considered for the electrical stimulation. On the right, the window corresponding to one of the applied boundary conditions is displayed.
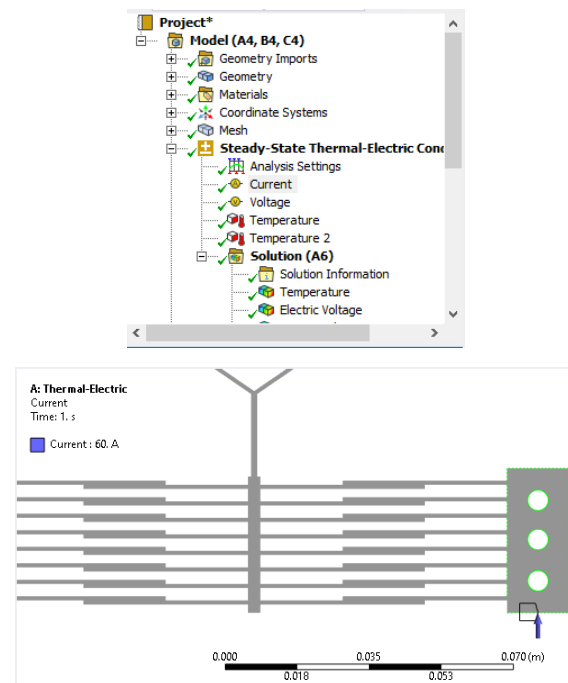
Figure 6. Graphical window showing the boundary condition relative to the current, with its maximum value.

As shown in Figure 7, a structural analysis was performed, linked to the Steady State Thermal analysis shown in Figure 6, with which the deformation generated by the displacement at the tips of the gripper is obtained. The boundary conditions are assigned as follows:

The Static Structural tool is coupled to Steady State Thermal, subsequently with the Fixed Support tool all the lateral faces of the anchors (actuator and gripper arms) are

selected and determined as fixed elements, in such a way that, by means of the thermoelectric effect, when applying to the current source, closing movement of the gripper is generated.

If the calculation of the reaction force is required, the movement of the tips of the gripper is restricted, a second Static Structural is used which is also coupled to the Steady State Thermal, then the fixed support of the first Static Structural is dragged, then, a second Fixed Support of the last Static Structural is selected to assign the restriction to the tips, this with the purpose of keeping them without movement to calculate the reaction force in the tips of the gripper. This is not our case since this experimental test is not considered. The assignments and boundary conditions can be seen in Figure 7, in the simulation tree and the graphical window.

3.2. Numerical results

To determine the boundary conditions, the experimentation and manufacturing of the gripper were carried out, because in the first comparisons large variations were observed, which were later reduced when considering the corresponding room temperature, obtaining a better approximation between the simulation and the experimentation. The current magnitude applied was also considered as a source of error.

Figure 8 shows two of 6 cases analyzed, where the temperature and the total deformation between the arms of the gripper are presented. The data of the simulation results with the room temperature of each of the 6 days (between June 16 and July 21) are shown in Table 4.
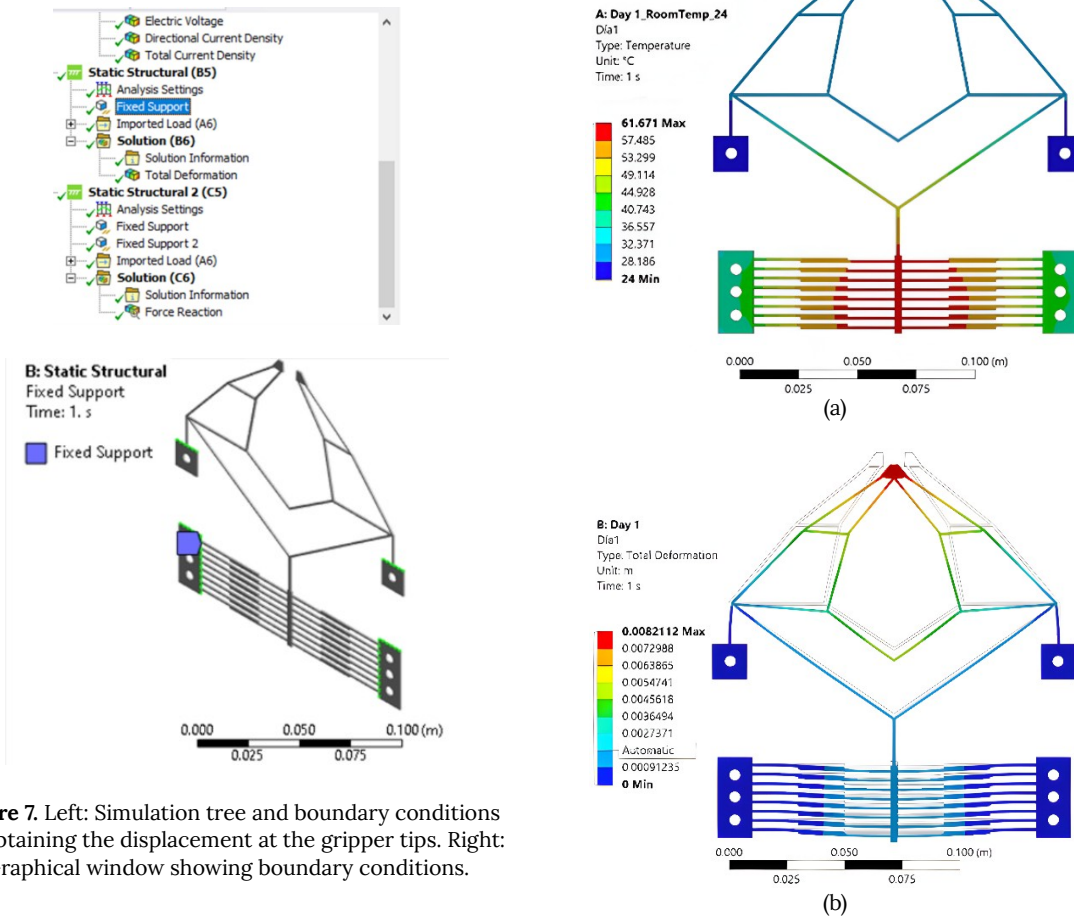
Figure 7. Left: Simulation tree and boundary conditions for obtaining the displacement at the gripper tips. Right: Graphical window showing boundary conditions.

(c)

(d)
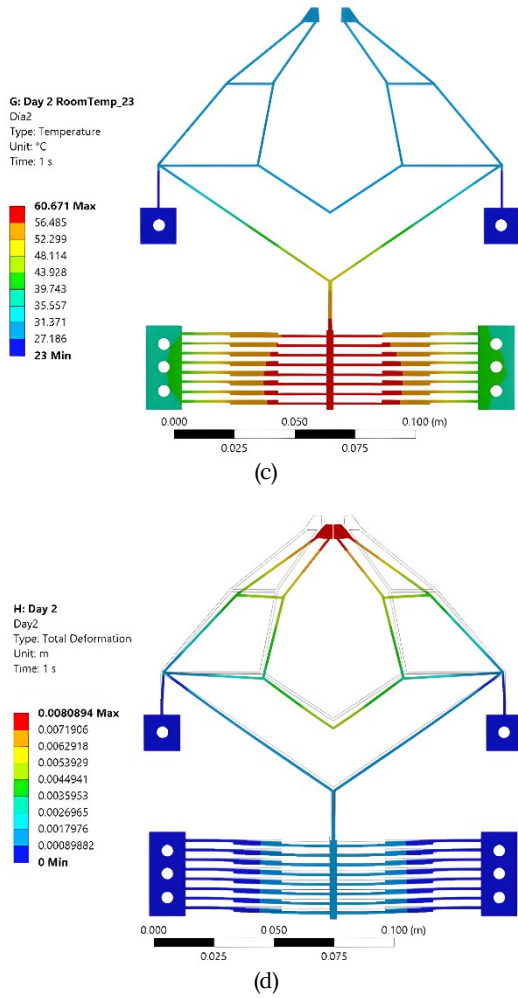
Figure 8. Temperature distribution temperature and displacement of the gripper when 60 A is applied. (a) and (b) Day 1, with 24°C was the room temperature. (c) y (d) Day 2, with 23°C was the room temperature.

**Table 4.** Magnitudes corresponding to temperature and displacement between jaws @ 60 A.

Day	Room temperature, (°C)	Shaft temperature, (°C)	Displacement between jaws, (mm)
1	24	61.671	8.211
2	23	60.671	8.089
3	21	58.671	7.792
4	24	62.671	8.386
5	23	61.671	8.237
6	23	60.671	8.089

From the data shown in Table 4, on average, the ambient temperature is 23°C, while the temperature at the shaft is 61°C and the displacement is 8.134 mm. Therefore, objects theoretically from 9 mm to approximately 0.8 mm in diameter can be clamped. Recall that the initial opening of the gripper corresponds to 9 mm.

4. FABRICATION OF THE GRIPPER IN ALUMINUM

Figure 9 shows the design made, with scaling, as well as the structure made on the aluminum plate.

(a)

(b)
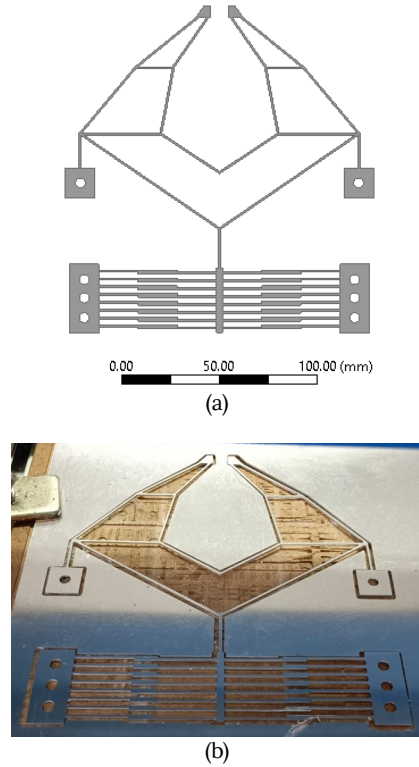
Figure 9. (a) Design, and (b) fabrication of the gripper.

In the manufacturing process, the geometry was exported in dxf2010 format. This file is opened in the Aspire software tool, where the internal and external cuts are profiled. Figure 10 shows the block diagram of the aluminum gripper manufacturing process.
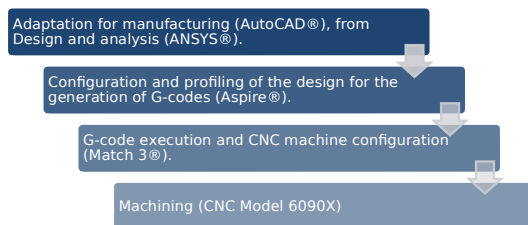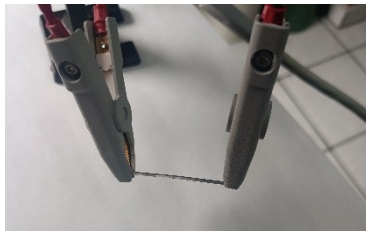

Figure 10. Fabrication process.

5. EXPERIMENTAL RESULTS

5.1 Aluminum resistivity, experimentally obtained

A rectangular aluminum probe with dimensions 1x1x40 mm was used, whose resistance of 1.83 mΩ was measured with a Keysigth Model E4980AL LCR equipment (Figure 11). From Ohm's Law, the magnitude of the resistivity is 4.33E-8 Ω·m.

(a)

(b)

Figure 11. (a) General experimental setup. (b) LCR measuring tips holding the element under testing.

5.2. Z-shaped chevron and complete gripper resistance

When the gripper was placed at its base to perform the experiment, due to the applied stresses, an effective opening of 10 mm was obtained, as shown in Figure 12.

Figure 12. Effective aperture of the gripper on its base.

The error percentages obtained from the theoretical, numerical, and experimental analysis of the resistance of the Z-shaped chevron actuator and the complete gripper are shown in Table 5. It can be observed that the approximation percentages are acceptable, based on the measurements in the LCR (Figure 13). It should be noted that, the actuator used in the measurement has slightly larger anchors, which contributes to the generation a slight difference, in relation to the measurement data.

(a)

(b)

Figure 13. Experimental setup to measure the resistance of (a) the Z-shaped chevron actuator, and (b) the gripper.

Table 5. Measured and calculated resistances.

Device	Experimental resistance (µΩ)	Analytical resistance (µΩ)	Error (%)	Numerical resistance (µΩ)	Error (%)
Z-shaped chevron actuator	559.23	555	0.71	N.D.	N.D.
Complete gripper	576.45	555	3.72	595.8	3.35

5.3. Experimental testing of the gripper

The experimental setup shown in Figure 14 was used to record the displacement, temperature distribution, and electric current of the microgripper. The elements of the experimental setup and the devices under test are:

1. Gripper, 2. Power source,
3. Industrial microscope, 4. Monitor,
5. Voltmeter, 6. Amperemeter,

7. Temperature sensor, and
8. Thermographic camera.

The images obtained with the thermographic camera allow visualizing the temperature distribution when applying an electric current intensity where the insulated clamp was fixed to avoid direct contact with a metallic structure used to avoid vibration, i.e. undesired movements. Subsequently, the source terminals were coupled to the actuator anchors. The data were used to perform the feedback and definition of the boundary conditions used in the simulations reducing the error between both approaches. The experiments were carried out for 6 days between June 16 and July 21. During this period there were no other people in the laboratory since they generated high variations in the measurements. That means that the metal prototypes are very sensitivity to temperature changes.

Temperatures on the shaft and the voltages generated in the actuator anchors were registered when applying the electric current sweep from 5 to 60 A, with 5 A steps. Figure 15 shows two representative cases where the temperature distributions observed with a thermographic camera are observed.
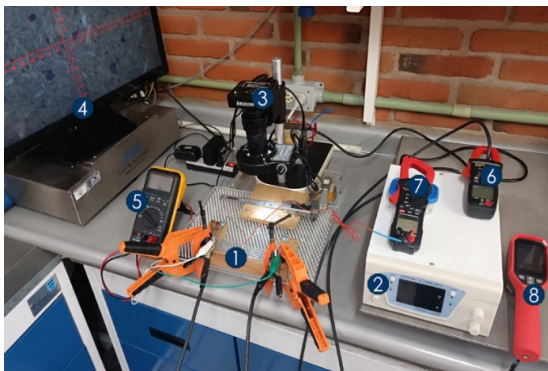

Figure 14. Experimental setup.

Experimental data were registered and compared with numerical ones as shows Figure 16.
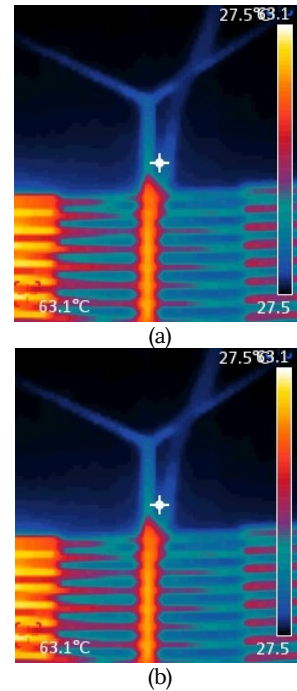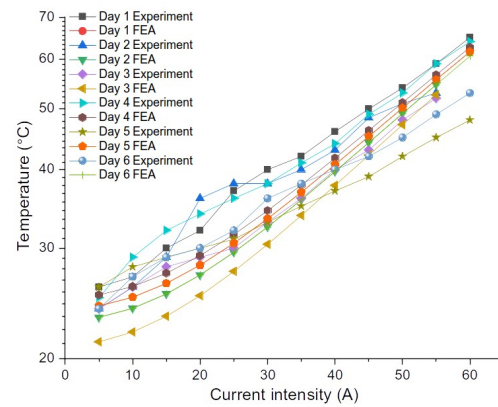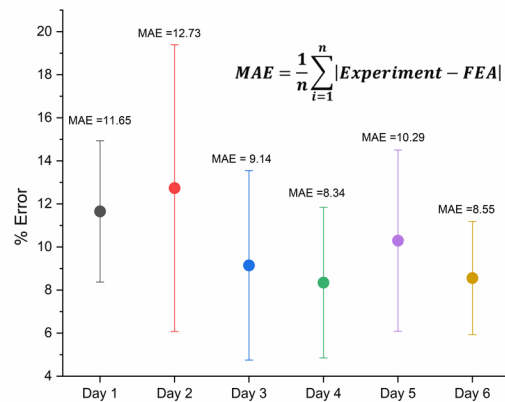

Figure 15. Thermographic camera images of temperature on the shaft. (a) Day 4, 63.1 °C, applying 60 A, and (b) Day 6, 32.5 °C, applying 20 A.
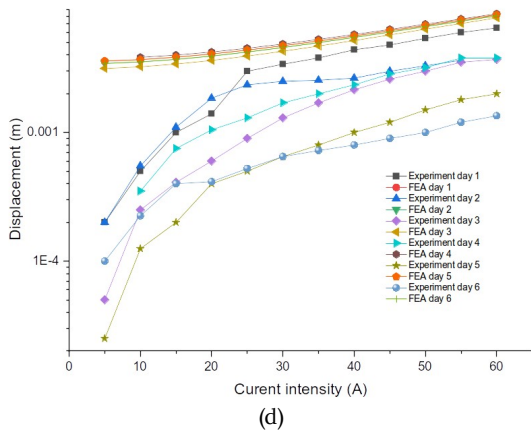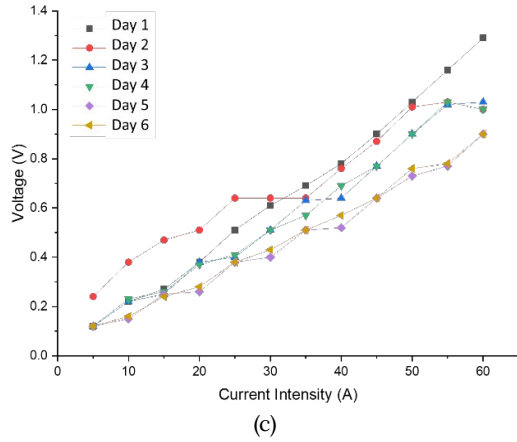

(a)

$$MAE = \frac{1}{n} \sum_{i=1}^{n} |Experiment - FEA|$$

(b)

(c)

(d)

Figure 16. (a) Shaft temperatures (numerical and experimental data), (b) average percentual error between numerical and experimental results on the temperature in the shaft (c) voltage generated in anchors (experimental data) (d) displacement between the tips of the gripper, numerical and experimental data.

The boundary conditions defined in the numerical analysis, obtained from the feedback with respect to the temperature of each day and the applied current, allow obtaining very close approximations in the shaft temperature, so that the average percentage error between the numerical and experimental shaft temperatures does not exceed 13%. Despite some inconveniences in the experimental tests, it was possible to get the deviation percentages closer, if air currents and people flow were avoided.

The temperature at the tips is not visible in the thermographic camera images since they remain practically at room temperature.

Which is very convenient to manipulate objects of different nature.

Regarding the voltage generation in the actuator anchors, it is observed that at 5 A there are variations between 0.1 and 0.22V, while at 60 A corresponds 0.9 and 1.3 V, so it is induced that, in case of applying voltage, the required levels are low. This kind of experimentation is planned to be done as part of future work.

Regarding the displacement of the gripper tips, the simulation results are extremely close, but in relation to the experimental ones, there is a significant variation, this fact can be attributed to external effects, since, although there were few people, there is no isolation booth. The trend, however, is similar in all cases. The average displacement at 60 A is 3.1mm. It implies that this gripper could clamp objects with diameters from 9 mm up to 5.9 mm in average. A representative image of the displacement between jaws are shown in Figure 17.
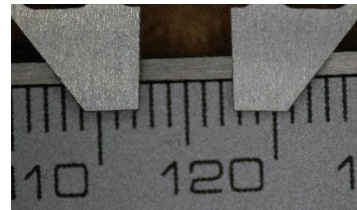
Figure 17. Image of the closing movement of the gripper using a microscope, 5.5 mm, applying 40 A.

6. CONCLUSIONS

This article provides the bio-inspired design of a microgripper considering silicon as structural material, which, for the purpose of validating the functionality of the geometry, at meso scale, is scaled for its fabrication in aluminum, presenting the results of its theoretical and numerical analysis, as well as its fabrication and experimental tests.

The most outstanding contributions of this work are the application of bioinspiration to create this novel design with a simple

configuration, low-cost materials, and easy fabrication process with a single structural material.

The parameters of interest are basically the shaft temperature and the displacement between its jaws. The experimental results of the temperature are sufficiently close to the theoretical ones since the average error does not exceed 13%. Regarding the initial and final opening, it is observed that objects with diameters from 9 mm to 5.9 mm can be gripped.

On the other hand, the fabrication and testing has highlighted the capability and applications in device characterization, as well as providing a visualization of performance, design improvement, and mechanical testing using accessible materials, such as aluminum. In addition, it has given us the opportunity to showcase the designs at exhibitions or scientific fairs thus giving visibility and creating more interest in the work done by observing the performance of scaled structures, which is expected to have a similar trend in the microstructures from which they were obtained.

As future work, it is planned to improve the experimental technique, including an isolation camera, to make experimental characterization tests with a higher degree of accuracy.

Acknowledgements

REFERENCES

[1] Chang, R. J., Lin, C. Y., Lin, P. S. Visual-Based Automation of Peg-in-Hole Microassembly Process. *Journal of Manufacturing Science and Engineering*. 2011, 133(4), doi: 10.1115/1.4004497.

[2] Nocentini, S., Parmeggiani C., Martella, D., Wiersma, D. S. Optically Driven Soft Micro Robotics. *Advanced Optical Materials*. 2018, 6(14), doi: 10.1002/adom.201800207.

[3] Lvu, Z., Qingsong, X. Recent design and development of piezoelectric-actuated compliant microgrippers: A review. *Sensors and Actuators A: Physical.* 2021, 331(1), doi:10.1016/j.sna.2021.113002.

[4] Franssila, S. *Introduction to microfabrication.* United Kingdom: John Wiley and Sons, 2010.

[5] Pustan, M., Chiorean, R., Birleanu, C., Dudescu, C., Muller, R., Baracu, A., Voicu, R. Reliability design of thermally actuated MEMS switches based on V-shape beams. *Microsyst Technol.* 2017, 23(1), 3863-3871, doi: 10.1007/s00542-015-2789-8.

[6] Biomimicry Institute. El proceso de diseño biomimético. Retrieved January 31, 2023, from https://toolbox.biomimicry.org/es/metodos/el-proceso-biomimetico.

[7] Guan, C., Yong, Z. An electrothermal microactuator with Z-shaped beams. *Journal of Micromechanics and Microengineering*. 2010, 20(8), doi:10.1088/0960-1317/20/8/085014.

[8] Volstad, N. L., Boks, C. Biomimicry – a useful tool for the industrial designer?. Norwegian university of science and technology. In: *Proc. of NordDesign 2008 Conf.*, Tallinn, Estonia, 2008, 275-284.

[9] Yoon, C. K. Advances in biomimetic stimuli responsive soft grippers. *Nano Convergence.* 2019, 6(20) (2019), doi:10.1186/s40580-019-0191-4.

[10] Soma, A., Iamoni, S., Voicu, R., Muller, R., Al-Zandi, M. H., Wang, C. Design and experimental testing of an electro-thermal microgripper for cell manipulation. *Microsystem Technologies*. 2017, 24(2), 1053–1060, doi: 10.1007/s00542-017-3460-3.

[11] Majidi Fard-Vatan, H., Hamedi, M. Design, analysis and fabrication of a novel hybrid electrothermal microgripper in microassembly cell. *Microelectronic Engineering*. 2020, 231(1), doi: 10.1016/j.mee.2020.111374

[12] «Aluminum 6053-T6». s. f. Retrieved July 26, 2023, from https://www.matweb.com/search/DataSheet.aspx?MatGUID=779d41ab5fc7444b8b7d965a178a5d81.

ACERCA DE LOS AUTORES

Alan J. Estrada Cabrera received the bachelor's degree in Mechatronics Engineering from the Universidad Tecnológica Emiliano Zapata, Mexico (2021). He is currently pursuing a master's degree in engineering and applied sciences (CIICAp-UAEM). His main research interests include MEMS, devices design using CAD, additive manufacturing, characterization techniques, and Bioinspiration.

Pedro Vargas Chable received the B. Sc. Degree by the Autonomous University Juarez from Tabasco in 2008. From 2009 to 2012, he was Technical Specialist Assessment of Lighting Conditions and Non-Ionizing Radiation, NOM-025-STPS-2008 and NOM-013-STPS-1993 respectively, in Environmental Technology S.A of C.V. In 2014 and 2019 he received the M.Sc. Degree and the Ph. D., respectively from the Autonomous University of Morelos State (UAEM). His current research interests are FEA, microgripper, microactuator design and characterization, and VLSI.

Margarita Tecpoyotl Torres received the Mathematician degree from the University of Puebla, Mexico (1991). She was also graduated as Electronic Engineer (1993). She received the M.Sc. and Ph.D. degrees in Electronics from National Institute of Astrophysics, Optics and Electronics, INAOE, México (1997 and 1999, respectively). Dr. Tecpoyotl works, since 1999, at UAEM, Mexico, where she is currently titular professor. She has been visiting research scientist at University of Bristol (2001), UK. She led the Winner team of Boot Camp, UAEM Potential, obtaining support to participate in Full Immersion Program, USA (2014). She was co-founder of INNTECVER (2014). She won the 3rd place in the Royal Academy of Engineering´s Leaders in Innovation Fellowships final pitch session, in UK (2015). Her main research interest includes MEMS, Antenna design, entrepreneurship, innovation; and development of educational programs. She holds the status of National Researcher (SNI), since 1999.

Ramon Cabello Ruíz received the Engineer Mechanical degree from the Autonomous University of the State of Morelos, Mexico (2010). He received the M. Eng. And Ph.D. degrees in Center for Research in Engineering and Applied Sciences, Mexico (2012 and 2017, respectively). He holds three SolidWorks certifications, (Mechanical Design level Associate, Mechanical Design level Professional, and Simulation level Associate). Dr. Cabello Works, since 2019, at UAEM, Mexico, where he is a part-time profesor. His area of expertise focuses on the design and mechanical analysis of microelectromechanical systems. He holds the status of National Researcher (SIN), since 2023.